

Atypical coupling between posterior regions of the default mode network in attention-deficit/hyperactivity disorder: a pharmaco-magnetoencephalography study

John D. Franzen, MD; Elizabeth Heinrichs-Graham, MA; Matthew L. White, MD;
Martin W. Wetzel, MD; Nichole L. Knott, R.EEGT; Tony W. Wilson, PhD

Franzen, Wetzel — Department of Psychiatry, University of Nebraska Medical Center, Omaha, Neb.; Franzen — Department of Psychiatry, Creighton University School of Medicine, Omaha, Neb.; Heinrichs-Graham, Knott, Wilson — Center for Magnetoencephalography, University of Nebraska Medical Center, Omaha, Neb.; Heinrichs-Graham — Department of Psychology, University of Nebraska, Omaha, Neb.; White — Department of Radiology, University of Nebraska Medical Center, Omaha, Neb.; Wetzel — Mental Health Unit, Lincoln Correctional Center, Nebraska Department of Correctional Services, Lincoln, Neb.; Wilson — Departments of Pharmacology & Experimental Neuroscience, and Neurological Sciences, University of Nebraska Medical Center, Omaha, Neb., USA

Background: Dysfunction in the default mode network (DMN), a group of cortical areas more active during the resting state, has been linked to attentional deficits and symptoms associated with attention-deficit/hyperactivity disorder (ADHD). Prior imaging studies have shown decreased functional connectivity between DMN nodes in patients with ADHD, primarily between anterior and posterior regions. Using magnetoencephalography (MEG), we evaluated phase coherence (i.e., functional connectivity) among regions of the DMN in healthy controls and adults with ADHD before and after stimulant therapy. **Methods:** We obtained a resting-state MEG recording for all participants. Magnetoencephalography data were transformed into a ~30 node regional source model using inverse spatial filtering, including regions corresponding to the DMN. We computed the zero-lag phase coherence between these regions pairwise for 5 distinct frequency bands, and we assessed group and medication effects. **Results:** Twelve adults with and 13 without ADHD participated in our study. Functional connectivity was stronger between particular node pairs and showed frequency-specific effects. Unmedicated patients showed reduced phase locking between posterior cingulate/precuneus regions (PCC) and right inferior parietal cortices (RIPL), and between medial prefrontal regions (MPFC) and the left inferior parietal region (LIPL) and the PCC. Unmedicated patients had increased phase locking between the RIPL and LIPL regions compared with controls. Administration of stimulants improved phase locking abnormalities along the MPFC–PCC and LIPL–RIPL pathways in patients with ADHD. **Limitations:** Modest sample size and lack of duration of patient treatment history may limit the generalizability of our findings. **Conclusion:** Adults with ADHD exhibit hyper- and hypoconnectivity between regions of the DMN during rest, which were suppressed after stimulant medication administration.

Introduction

Attention-deficit/hyperactivity disorder (ADHD) is one of the most common neurobehavioural disorders, affecting 8% of children and persisting in 4% of adults in the United States.¹ Cardinal symptoms of ADHD include inattention, motor restlessness and impulsivity,² which often lead to educational and occupational impairments.³ Considering the in-

dividual and societal burdens associated with ADHD, gaining a better understanding of what causes ADHD and elucidating the underlying mechanisms of applicable medications is an important focus of clinical neuroscience research.

A large corpus of normative studies has identified a group of brain areas, the default mode network (DMN), that appear to be more active when participants are in an awake resting state compared with a cognitively active state. Raichle and

Correspondence to: T.W. Wilson, Department of Pharmacology and Experimental Neuroscience, University of Nebraska Medical Center, 988422 Nebraska Medical Center, Omaha NE 68198, United States; tony.w.wilson@gmail.com

J Psychiatry Neurosci 2013;38(5):333-40.

Submitted Mar. 14, 2012; Revised Sept. 20, Nov. 26, 2012; Accepted Feb. 12, 2013.

DOI: 10.1503/jpn.120054

colleagues⁴ coined the term “default mode,” referring to the brain’s intrinsic activity when a person is at rest, which has been associated with processes such as self-reflection and mind wandering. Areas of the DMN include the medial prefrontal cortex (mPFC), the posterior cingulate/precuneus cortices (PCC) and the mediolateral inferior parietal cortices bilaterally (RIPL and LIPL).^{5,6} These areas were noted to be more active and to exhibit increased functional connectivity at rest in healthy adults.⁴ Interestingly, areas of the DMN also appear to have an inverse correlation with task-oriented brain regions. They exhibit robust deactivations when attentional and other networks are strongly active (e.g., during an attention task) and become reactivated when processing in task-oriented cortices subsides.⁷

Previous studies have evaluated multiple facets of the DMN and its possible dysfunction in patients with ADHD. Based on functional magnetic resonance imaging (fMRI) studies, circumscribed brain areas are known to exhibit inter-regional correlations at very low frequency (i.e., functional connectivity) across distinct functional networks, including the DMN.⁷⁻⁹ Using fMRI, Greicius and colleagues¹⁰ were able to identify specific regions of the DMN, including the PCC and mPFC, that demonstrated an increase in functional connectivity during a resting state compared with performance of a working memory task in healthy adults. Dysfunction in the DMN, specifically the inability to effectively deactivate the DMN, may cause interference during task-positive activities, and has been linked to attentional lapses and longer reaction times in those with ADHD.^{11,12} Decreased network homogeneity, a measure of network-wide functional connectivity, has also been found in the DMN of those with ADHD.^{13,14} However, Castellanos and colleagues¹⁵ observed more limited aberrations in ADHD, such as decreased functional connectivity between the mPFC and PCC regions. They also argued that given the anatomic abnormalities observed in their earlier work,¹⁶⁻¹⁸ the PCC region should be considered the possible locus of dysfunction in patients with ADHD. Moreover, fMRI studies have linked stimulant medication, the most efficacious treatment for ADHD, to normalization of activity between medial prefrontal areas and posterior cingulate cortices of the DMN in youths with ADHD.^{19,20}

Although most DMN and more general resting-state studies have used fMRI techniques, several recent studies have begun to characterize the electrophysiological basis of these networks using magnetoencephalography (MEG).²¹⁻²⁴ These electrophysiological studies have identified roughly the same brain networks found with fMRI and have shown that these networks are more dominant in the Δ , θ , α and low β frequency bands in healthy adults. However, to our knowledge, the electrophysiological basis of resting-state networks, including the DMN, has not been examined in patients with ADHD. In the present study, we quantified phase coherence in the DMN to examine inter-regional connectivity at ultra-low (< 2.0 Hz), Δ , θ , α and β frequencies using MEG, a direct measure of neurophysiology. Coherence measures, commonly interpreted as a gauge of inter-regional communication or interaction, have been widely used to quantify phase and/or amplitude similarities between neuronal oscil-

lations.^{25,26} Phase coherence specifically can be interpreted as a measure of phase consistency between distinct brain areas across recorded time series data.²¹ Briefly, we evaluated zero-lag phase coherence among the 4 primary nodes of the DMN in unmedicated and medicated adults with ADHD, and in an evenly matched sample of healthy controls. Our key hypotheses were that adults with ADHD would exhibit decreased functional connectivity between DMN regions, and that this dysfunction would be normalized with stimulant therapy.

Methods

Participants

We studied adults with the inattentive subtype of ADHD and a group of healthy controls matched for age, sex, years of education and race. All participants with ADHD had shown a satisfactory clinical response to a mixture of dextroamphetamine salts, extended release formula (MAS-XR; Adderall XR), and had been prescribed the same regularly monitored dosage for at least 6 months before study enrolment. Patient diagnoses were based on a semistructured comprehensive psychiatric assessment by a board-certified psychiatrist (M.W.W.) using DSM-IV diagnostic criteria, the Adult ADHD Self-Report Scale²⁷ and collateral history, with the diagnosis of ADHD being the primary Axis I diagnosis. Of note, control participants did not meet DSM-IV criteria or meet the threshold on the Adult ADHD Self-Report Scale for the diagnosis of ADHD. Exclusion criteria were any medical illness affecting central nervous system function, neurologic disorder, history of head trauma and current substance abuse. Participants provided written informed consent after receiving a complete description of the study. The Institutional Review Board at the University of Nebraska Medical Center approved our study protocol.

Experimental paradigm

All participants were scheduled for MEG early in the morning (e.g., 07:30–08:00) and, for the group with ADHD, a minimum of 18 hours since their last stimulant dosage. On arrival, each participant was positioned inside the MEG room and completed a 6-minute block of awake, eyes-closed rest. We instructed participants to relax but remain awake with their eyes closed until a study staff member told them the scan was complete. Participants with ADHD then received their standard dosage of MAS-XR and moved to the patient waiting area. About 75 minutes later, they returned to the MEG room and completed a second (identical) block of awake, eyes-closed rest.

MAS-XR is an extended-release amphetamine product approved by the United States Food and Drug Administration for the treatment of ADHD in adults. It combines neutral sulfate salts of dextroamphetamine and amphetamine, with the dextro isomer of amphetamine saccharate and d,l-amphetamine aspartate monohydrate. When administered, blood plasma concentration levels rise sharply then begin to

asymptote toward a peak of 20–30 ng/mL at 6–8 hours postadministration. This is followed by a gradual decline in plasma concentration level over the next 16–18 hours. However, the degree to which the brain's response curve follows the plasma concentration curve is entirely unknown.

Structural MRI

We acquired high-resolution neuroanatomic images using a Philips Achieva 3 T X-series scanner. The T_1 -weighted sagittal images were obtained with an 8-channel head coil using a 3-dimensional fast field echo sequence with the following parameters: field of view 24 cm, slice thickness 1 mm with no gap, in-plane resolution 1.0×1.0 mm, sense factor 1.5. The structural volumes were aligned parallel to the anterior and posterior commissures and used for MEG coregistration.

MEG data acquisition

All recordings took place in a 1-layer magnetically shielded room with active shielding engaged. With an acquisition bandwidth of 0.1–330 Hz, neuromagnetic responses were sampled continuously at 1 kHz using an Elekta Neuromag system with 306 magnetic sensors. Using MaxFilter (v2.1.15; Elekta), MEG data from each session and participant were transformed into a standard device-centred head position, individually corrected for head motion, coregistered to structural MRI and subjected to noise reduction using the signal space separation method with a temporal extension (tSSS).^{28,29}

MEG source analyses

After tSSS and head-motion correction, we divided the sensor-level time series into epochs of 4096 ms duration (4096 points) and performed artifact rejection using a fixed threshold method supplemented with visual inspection. We then transformed artifact-free epochs for each condition and participant into a regional source model via inverse spatial filtering using the Brain Electrical Source Analysis software (BESA version 5.3.2; Fig. 1).^{30,31} Essentially, a 29-point grid with dual orthogonal orientations per point was constructed using a standard model in BESA, and spatial filtering was performed by creating a linear inverse operator of the lead field matrix $L = (l_1, l_2, \dots, l_n)$, which contained the lead field vector of each source orientation in the model. Briefly, we can denote the MEG signals from the individual sensors by the matrix U (sensors \times samples) and state that U is the linear overlap coming from the source regions (i.e., $U = L \times S + \text{noise}$), with each source region having an unknown level of activity over time (s_i , row i in source time series matrix S). The unknown levels of brain activity S can then be reconstructed by inverting matrix L (i.e., $S = L^{-1} \times U - L^{-1} \times \text{noise}$), with L^{-1} being a spatial filter that reconstructs the magnitude of source activity in brain area i over time (s_i) while suppressing activity from all other brain areas. We used regularization (1%), based on the truncated singular value decomposition approach, to prevent the weights in the inverse spatial filter operator (L^{-1}) from becoming too large and enhancing the

MEG background noise. Such regularization causes some minor smearing of activity among the sources. Overall, this reconstruction method closely follows that described by Scherg and colleagues.³⁰

After transformation into source space, we transformed the current–amplitude (nAm) time series for each of the 2 orthogonal orientations per source into the time–frequency domain using complex demodulation.³² We then extracted the zero-lag phase-locking value (PLV), using the method described by Lachaux and colleagues,³³ for the dominant orientation of each source corresponding to the 4 regions of the DMN in reference to each of the other 28 brain regions. Briefly, the signals were band-pass filtered at ± 0.5 Hz, and their convolution was computed using a complex Gabor wavelet centred at the target frequency. We extracted the phase of the convolution for each time bin, trial and source pair and then averaged these

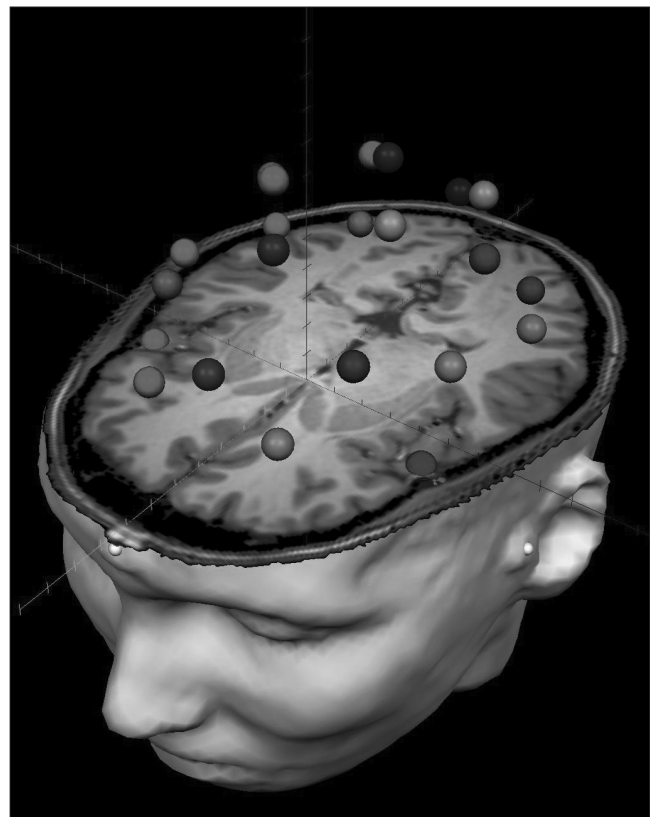


Fig. 1: Example of the 29-node regional source model. For each participant, a 29-node model was fitted to their magnetic resonance imaging (MRI) scan after coregistration, and this model was used to estimate regional neuronal activity during the resting-state recording using inverse spatial filtering. The model can be seen overlaid on the MRI of a patient with attention-deficit/hyperactivity disorder. The distinct shades visually distinguish the regional sources. Note that sources are spaced equidistantly and that each represents neural activity over an extended cortical area (i.e., $> 1 \text{ cm}^3$). Each node's time series reflects the average neuronal activity over that brain region and not the amount of activity at a precise anatomic coordinate (e.g., a voxel in Montreal Neurological Institute space). The 4 nodes corresponding to default mode network regions were the focus of all statistical analyses of the present study.

values across trials to derive the PLV, which we then collapsed across the time bins of the 4096 ms epoch to estimate the average PLV per source or node pair. Thus, the PLV reflects the intertrial variability of the phase difference across the entire epoch. Values close to 1 indicate that the phase difference across trials (at a given frequency) varies only minutely, whereas values close to 0 indicate substantial phase variation between the 2 signals across trials. Finally, for each source, we considered the orientation with greater broadband spectral power across the entire resting recording to be the dominant orientation, and we used this orientation for all PLV analyses.

Based on previous studies^{4-15,19-24} and our hypotheses, we examined phase-locking between nodes of the DMN within the Δ (1.5–4 Hz), θ (4–7.5 Hz), α (8–13 Hz), β (14–22 Hz) and an ultra-low frequency bands (< 2.0 Hz) using mixed-model analyses of variance (ANOVA) per frequency band. Initially, we evaluated

group differences using ANOVAs with DMN pathways (6 in total) as a within-subjects factor, and group (with/without ADHD) as a between-subjects factor. Subsequently, we examined medication effects using repeated-measures ANOVAs, with pathways and treatment status (pre/post) as within-subjects factors. Statistical analyses were conducted in SPSS for Windows (release 11.0.1). For all MEG preprocessing and source modelling, we used the BESA (version 5.3.2) software, and for MEG–MRI coregistration and visualization, we used the BrainVoyager QX (version 2.2) software.

Results

Twelve adults (4 women) with the inattentive subtype of ADHD and 13 adults (4 women) without ADHD participated in the study. Mean ages were 40.58 (standard deviation [SD] 12.1) years in the ADHD group and 40.92 (SD 10.7) years in

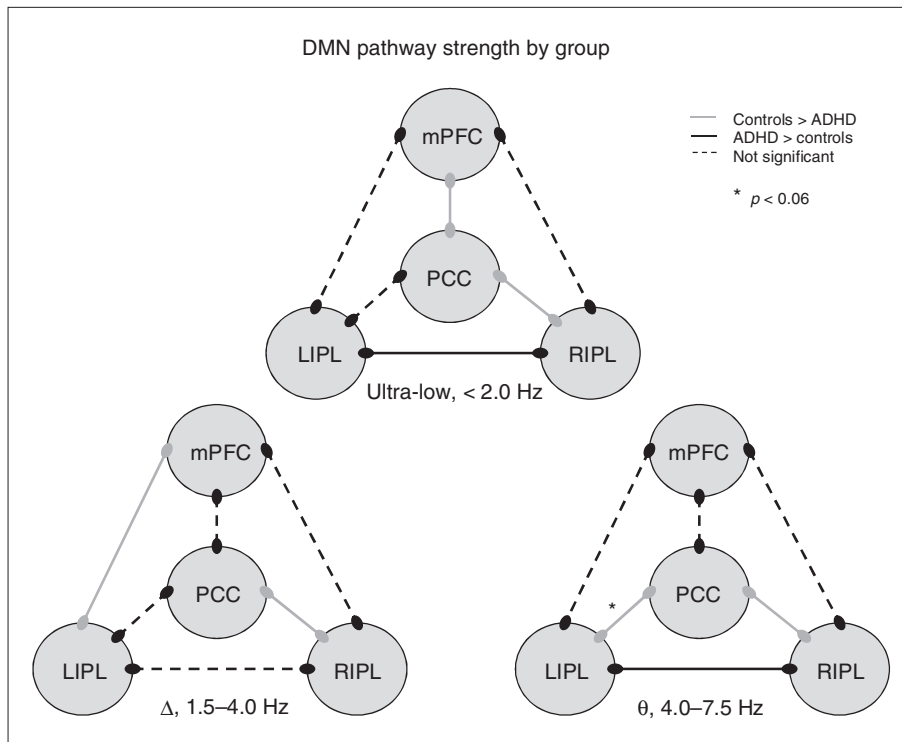


Fig. 2: Functional connectivity in the default mode network (DMN) of unmedicated adults with and without attention-deficit/hyperactivity disorder (ADHD). Three models of the DMN showing group differences and similarities in functional connectivity along particular pathways at distinct frequencies of neuronal firing are shown. In the ultra-low frequency range, adults without ADHD showed stronger coupling between the medial prefrontal cortex (mPFC) and posterior cingulate/precuneus (PCC) regions and between the PCC and right medial lateral inferior parietal cortices (RIPL) areas, whereas those with ADHD showed stronger connectivity between the posterior RIPL and left medial lateral inferior parietal cortices (LIPL) nodes. In the Δ band, controls showed increased connectivity between the mPFC and LIPL regions and the PCC and RIPL regions relative to unmedicated patients with ADHD. The θ frequency neuronal activity was more strongly coupled between the PCC region and the RIPL and LIPL areas in adults without ADHD relative to their peers with ADHD, whereas the latter group showed stronger coupling between the RIPL and LIPL cortical areas. Interestingly, the increased functional connectivity in the PCC–RIPL pathway of adults without ADHD was consistent throughout all 3 frequency ranges of neuronal firing. Note that α activity is not shown as there were no group differences in coupling strength along any pathways.

the control group at the time of enrolment. One participant with ADHD was left-handed and all others were right-handed. Each group had 1 Latino participant, and the remaining participants were white.

We initially evaluated the 29-node regional source model to confirm the presence of DMN activity. Since we expected DMN activity to be abnormal in people with ADHD, this analysis was restricted to adult control participants. We used the PCC as the seed region for this analysis, because this node is generally the most robust (e.g., in fMRI studies). Briefly, we computed the average PLV between the PCC and the other 3 DMN regions and between the PCC and all non-DMN regions for each frequency band. These data were then evaluated using paired *t* tests. The results indicated that, for each of the 5 frequency bins, phase-locking was significantly stronger between the PCC and other DMN regions relative to non-DMN regions (all $p < 0.01$).

MEG data: between-group comparisons

The mixed-model ANOVA for phase coherence in the ultra-low frequency band (< 2.0 Hz) indicated a main effect of pathway ($F_{5,115} = 17.55, p < 0.001$) and a pathway \times group interaction ($F_{5,115} = 3.8, p = 0.003$; Figs. 2 and 3). The main effect of group was not significant. Given the interaction effect, follow-up testing of the main effect of pathway, which was not our primary focus, was performed separately for each group and reported as supplementary data (Appendix 1, available at cma.ca/jpn). The pathway \times group interaction effect reflected stronger phase-locking between the PCC–RIPL ($p = 0.042$) and mPFC–PCC ($p = 0.035$) in controls, and stronger LIPL–RIPL phase-locking in the unmedicated adults with ADHD group ($p = 0.038$; Figs. 2 and 3).

The ANOVA for PLVs in the Δ band (1.5–4.0 Hz) showed a main effect of pathway ($F_{5,115} = 12.85, p < 0.001$) and a pathway \times group interaction effect ($F_{5,115} = 2.44, p = 0.038$; Figs. 2 and 3). The main effect of group was not significant. Again, the main effect of pathway was not the primary focus of this study, and post hoc testing of this effect can be found in Appendix 1. Follow-up *t* tests of the group \times pathway interaction term revealed that controls had significantly greater phase-locking between mPFC–LIPL ($p = 0.043$) and PCC–RIPL ($p = 0.019$) than the unmedicated ADHD group (Figs. 2 and 3).

Statistical testing of the θ range (4.0–7.5 Hz) showed a main effect of pathway ($F_{5,115} = 6.46, p < 0.001$), an interaction effect ($F_{5,115} = 3.92, p = 0.005$) and no group main effect (Figs. 2 and 4). Post hoc testing of the pathway main effect is reported as supplementary data in Appendix 1. The interaction term reflected greater phase-locking between the PCC–RIPL in the control group ($p = 0.026$) and between the LIPL–RIPL in the unmedicated ADHD group ($p = 0.049$). There was also a strong trend in the PCC–LIPL pathway (ADHD $<$ controls, $p = 0.06$).

Finally, the ANOVAs for α -band (8.0–13.0 Hz) and β -band (14–22 Hz) phase-locking indicated a main effect of pathway ($F_{5,115} = 7.80, p < 0.001$), without a main effect of group or an interaction effect (Fig. 4). Follow-up testing is discussed in Appendix 1.

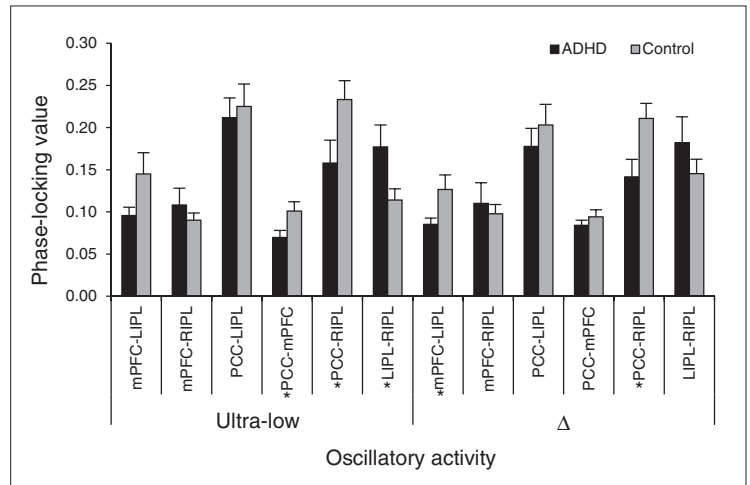


Fig. 3: Phase coherence: slow oscillatory activity in the default mode network (DMN). Phase-locking values (PLVs) of each node pair in the DMN of unmedicated adults with attention-deficit/hyperactivity disorder (ADHD; black) and controls (grey) are grouped together along the x axis by frequency band (left: ultra-low activity; right: Δ band activity). The y axis reflects group mean PLVs, which vary from 0 (no phase-locking) to 1 (perfect phase-locking). Group differences varied by pathway and, within a particular pathway, by the frequency of coherent firing activity between neuronal populations. Asterisks identify individual node pairs where significant differences between unmedicated adults with ADHD and controls were observed. Error bars indicate 1 standard error of the mean.

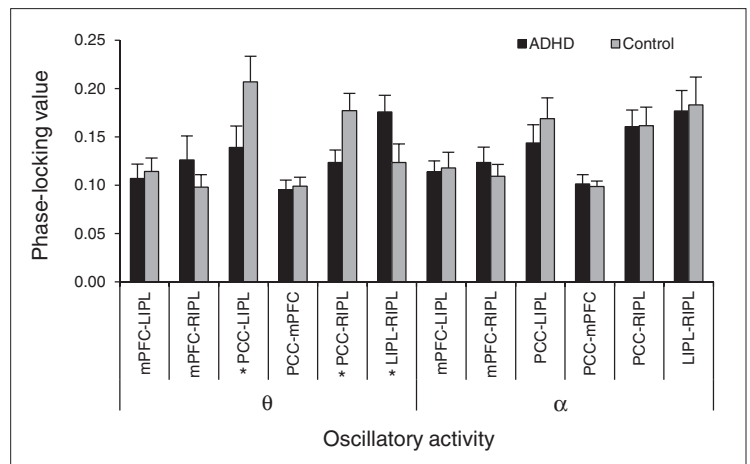


Fig. 4: Phase coherence: θ and α oscillatory activity. The phase-locking value (PLV) group means for each node pair are represented by black and grey colours and grouped together along the x axis by frequency range. The y axis depicts the PLV, which varies from 0 to 1. Group differences by pathway were found for population-level θ activity, but not α frequency discharges. Asterisks highlight the node pairs where significant differences were found between unmedicated adults with attention-deficit/hyperactivity disorder (ADHD) and controls. Error bars indicate 1 standard error of the mean.

MEG data: MAS-XR treatment effects

The DMN pathways that suggested aberrant interactions in the between-group comparisons were probed with paired and independent *t* tests to evaluate the therapeutic effects of MAS-XR administration. These analyses indicated a significant increase in ultra-low frequency phase-locking in the mPFC–PCC pathway following MAS-XR treatment in adults with ADHD ($t_{11} = -6.58, p < 0.001$). No other pre- or post-treatment (within-group) effects were significant, but between-group comparisons using the posttreatment ADHD data indicated that all significant pathway \times group interaction effects had dissipated. Thus, MAS-XR administration in adults with ADHD increased phase-locking in some pathways (mPFC–PCC, mPFC–LIPL, PCC–LIPL, PCC–RIPL) and decreased it in other pathways (LIPL–RIPL), depending on the nature of the initial perturbation.

Discussion

We evaluated inter-regional interactions within the DMN of adults with and without ADHD. Within each group, we observed a distinct hierarchy of inter-regional coupling strengths among the 6 node pairs that compose the DMN. Furthermore, these group-specific hierarchies varied by frequency range, which suggests that distinct node pairs may use specialized population-level neuronal firing rates to ensure the veracity of their interactions, and that such rate codes may be perturbed in adults with ADHD. Of special interest, we observed group differences along particular pathways. In controls, functional connectivity was significantly stronger between the PCC–RIPL nodes (ultra-low, Δ and θ bands), mPFC–LIPL (Δ band) and mPFC–PCC (ultra-low band) and trended between the PCC–LIPL (θ band) node pairs. In the group with ADHD, functional connectivity was more robust between the LIPL–RIPL nodes in the ultra-low and θ frequency bands. Finally, medication effects were apparent in the group with ADHD. Although these findings should be considered preliminary, the stimulant medications appeared to suppress aberrant functional connectivity by increasing phase-locking in some pathways and decreasing it in others. We discuss these findings in light of DMN studies in healthy individuals, the implications of our pathway-specific findings and areas to consider for future studies.

Along with decreased DMN functional connectivity, people with ADHD appear to exhibit decreased global brain efficiency.³⁴ Global brain efficiency is a measure of network topology that is thought to reflect the number of long-range structural connections.³⁴ Wang and colleagues³⁴ demonstrated that children with ADHD exhibited a decrease in global brain efficiency and an increase in local brain efficiency, which together produced a shift in the ADHD brain toward a more regular network topology and away from the classic small world topology found in their group of healthy children. Interestingly, our study found an increase in functional connectivity in the IPL bilaterally that may suggest an increase in local efficiency in adults with ADHD. While not the primary purpose of our study, interactions between these secondary

brain regions may represent a more locally efficient alternative pathway than the mPFC–PCC path of the DMN in healthy people. One possible theory for this is that dysfunction in the mPFC–PCC pathway produces a deficiency in the mPFC's ability to downregulate posterior regions, including the RIPL and LIPL, and that this affects functionality across the entire DMN. Such a deficit in the capacity of frontal regions to regulate (up or down) posterior cortices would be consistent with the overall symptomatology of ADHD, including inattention. However, unfortunately the PLV is only a measure of correlation and does not allow one to draw strong conclusions regarding the direction of regional interactions. Although this interpretation would appear to be consistent with the results of a recent meta-analysis, which identified hypoactivation in executive function networks and hyperactivation in the DMN and visual networks.³⁵ These findings highlight a pattern of increased and decreased activation in ADHD, which appears to roughly follow (with some irregularities) the task-positive and task-control networks.^{7,10} Future studies should evaluate both functional connectivity and activation magnitude in these networks, and conduct network-level analyses to determine whether an imbalance or aberrant interaction between task-positive and task-negative networks has explanatory power for this overall set of findings.

Interestingly, the DMN is thought to undergo a maturation process from childhood to adulthood,^{36,37} and abnormalities in this process may play a role in the development of dysfunctional connectivity for those with ADHD. This aberrant functional connectivity within the DMN may be a corollary of abnormal neuronal pruning or abnormal myelination and should be considered as a possible area for future research. A variety of studies have demonstrated abnormal functional connectivity in the DMN of people with ADHD, which is consistent with our findings. While most studies have shown hypoconnectivity in the DMN,^{13–15} there have been studies suggesting hyperconnectivity^{38,39} involving specific regions of the DMN. Our study seemed to be consistent with both findings. Essentially, we found decreased functional connectivity along the mPFC–PCC and PCC–RIPL pathways and an increase between the LIPL–RIPL nodes in people with ADHD compared with controls. These findings appear to be consistent with both hyperconnectivity between posterior DMN nodes and hypoconnectivity among the long-range anterior–posterior aspects of the DMN. This dysfunction in the DMN may account in part for attentional lapses and other symptoms associated with ADHD. It should be noted that our primary findings were largely outside of what is thought to be the dominant band (α band) for DMN activity in healthy adults.²² Basically, we found no group differences or medication effects for α activity, which may indicate that people with ADHD have a more subtle abnormality in DMN function and regional interactions within the network.

Besides functional abnormalities, previous studies have shown altered brain structure in areas of the DMN in people with ADHD. Volumetric aberrations, such as reduced prefrontal and anterior cingulate cortical volumes, and lower overall cortical grey matter volume have been noted in people

with ADHD.⁴⁰ These specific areas of the brain are noted to be important in attention and executive decision-making. Meanwhile, diffusion tensor imaging studies have shown deficits in structural connectivity. Silk and colleagues⁴¹ demonstrated abnormalities in the frontoparietal tracts of children with ADHD that normalized with age, which may indicate a possible delay in neural maturation. A recent longitudinal MRI study evaluating peak cortical thickness, the instant where growth is followed by a decline in thickness, reached a similar conclusion, demonstrating that children and adolescents with ADHD reached this point much later than controls.⁴² Interestingly, the brain areas most prominently affected by these delayed maturational effects were regions of the prefrontal cortex.⁴² This same group⁴³ of investigators evaluated participants with ADHD whose clinical symptoms improved over time and those whose symptoms did not improve compared with controls. At baseline, thinning of the left medial prefrontal cortex and cingulate brain regions was observed in participants with worse clinical outcomes (i.e., those whose symptoms did not improve over time) compared with participants with good outcomes and controls. Moreover, participants with better outcomes (i.e., symptoms improved over time) exhibited a distinct cortical thickness trajectory in the right parietal lobe compared with those with worse outcomes and controls. Children whose outcomes improved over time showed significantly decreased cortical thickness in the right parietal lobe at baseline compared with controls, but cortical thickness in this area had normalized compared with controls by the follow-up scan during adolescence (about 6 years later). This normalization can be argued as a mechanism for the improved clinical outcomes. Similar structural findings, including cortical thinning of the right inferior parietal lobe, dorsolateral prefrontal and anterior cingulate cortices, have been shown in adults with ADHD compared with healthy adults.⁴⁴ Findings from these structural studies further strengthen the argument that the underlying pathophysiology of ADHD includes abnormalities in regions of the DMN.

Limitations

Our study has several limitations that are important to recognize, as they restrict the generalizability of the findings. These include modest sample sizes, distinct medication histories of participants with ADHD (e.g., duration of treatment), the lack of a placebo control group, potential confounds with computing connectivity values and alternative interpretations of our findings. One important issue to acknowledge is that our finding of a normalization of PLVs in the ADHD group following medication administration could simply reflect regression to the mean. With respect to computing the PLV, it is important to recognize that the amplitude of the signal (i.e., the signal-to-noise ratio) can bias the obtained PLV and that a change in the amplitude of a signal (e.g., between 2 conditions) can masquerade as a change in the PLV. We examined this potential confound with estimations of the PLV in our data, but the possibility that this affected our results can never be entirely ruled out. Moreover, signal leak-

age can also bias connectivity estimations, especially in brain regions located proximal to the seed region. Since seed regions were always spatially distant from the target regions in this study, it is unlikely that signal leakage significantly affected our results; however, this possibility cannot be entirely eliminated, as such leakage is also highly inhomogeneous. To our knowledge, only 1 imaging study²⁰ to date has used both a healthy control group and a placebo treatment group, and the same 13 children were included (at 2 different time points) to form the placebo and treatment groups. Thus, future work will need to examine larger and more homogeneous patient groups, include placebo treatment and healthy control comparison groups and extend the current observations to younger people with ADHD.

Conclusion

Our study demonstrated aberrant phase-locking between regions of the DMN in people with ADHD, which was marginalized by the administration of stimulant medications. We identified distinct functional pathways between node pairs, including the mPFC–PCC and the LIPL–RIPL, that appear to function in opposition to each other in those with ADHD. While these findings augment our understanding of the underlying pathophysiology of ADHD and the pharmacologic effects of stimulant medications, further research is needed to fully understand the disease process and the factors that modulate it.

Acknowledgements: Funding for the Center for Magnetoencephalography has been generously provided by an anonymous private donor. E. Heinrichs-Graham was supported by the Hattie B. Munroe Foundation through a graduate research assistantship.

Competing interests: None declared by J.D. Franzen and N.L. Knott. As above for E. Heinrichs-Graham. M.L. White reported consulting fees from Philips Healthcare, serves on the advisory board for Bayer HealthCare Pharmaceuticals Inc., and has received grant funding from Bracco Diagnostics Inc. M.W. Wetzel has received speaker honoraria from Shire. T.W. Wilson receives grant funding through his institution from the National Institutes of Health. The funders had no role in study design, data collection and analysis, decisions to publish, or preparation of the manuscript.

Contributors: M.W. Wetzel and T.W. Wilson designed the study. E. Heinrichs-Graham and T.W. Wilson acquired the data. J.D. Franzen, E. Heinrichs-Graham, M.L. White and T.W. Wilson analyzed the data. J.D. Franzen, E. Heinrichs-Graham and T.W. Wilson wrote the article. E. Heinrichs-Graham, M.L. White, M.W. Wetzel, N.L. Knott and T.W. Wilson reviewed the article. All authors approved its publication.

References

1. Center for Disease Control and Prevention (CDC). Mental health in the United States: Prevalence of diagnosis and medication treatment for attention-deficit/hyperactivity disorder — United States, 2003. *MMWR Morb Mortal Wkly Rep* 2005;54:842-7.
2. American Psychiatric Association. *Diagnostic and statistical manual of mental disorders*. 4th ed., text revised. Washington: The Association; 2000.
3. Biederman J, Faraone SV. The effects of attention-deficit/hyperactivity disorder on employment and household income. *MedGenMed* 2006;8:12.

4. Raichle ME, MacLeod AM, Snyder AZ, et al. A default mode of brain function. *Proc Natl Acad Sci U S A* 2001;98:676-82.
5. Schilbach L, Eickhoff SB, Rotarska-Jagiela A, et al. Minds at rest? Social cognition as the default mode of cognizing and its putative relationship to the "default system" of the brain. *Conscious Cogn* 2008;17:457-67.
6. Konrad K, Eickhoff SB. Is the ADHD brain wired differently? A review on structural and functional connectivity in attention deficit hyperactivity disorder. *Hum Brain Mapp* 2010;31:904-16.
7. Fox MD, Snyder AZ, Vincent JL, et al. The human brain is intrinsically organized into dynamic, anticorrelated functional networks. *Proc Natl Acad Sci U S A* 2005;102:9673-8.
8. Fransson P. Spontaneous low-frequency BOLD signal fluctuations: an fMRI investigation of the resting-state default mode of brain function hypothesis. *Hum Brain Mapp* 2005;26:15-29.
9. De Luca M, Beckmann CF, De Stefano N, et al. fMRI resting state networks define distinct modes of long-distance interactions in the human brain. *Neuroimage* 2006;29:1359-67.
10. Greicius MD, Krasnow B, Reiss AL, et al. Functional connectivity in the resting brain: a network analysis of the default mode of brain function. *Proc Natl Acad Sci U S A* 2003;100:253-8.
11. Weissman DH, Roberts KC, Visscher KM, et al. The neural bases of momentary lapses in attention. *Nat Neurosci* 2006;9:971-8.
12. Sonuga-Barke EJ, Castellanos FX. Spontaneous attentional fluctuations in impaired states and pathological conditions: a neurobiological hypothesis. *Neurosci Biobehav Rev* 2007;31:977-86.
13. Uddin LQ, Kelly AM, Biswal BB, et al. Network homogeneity reveals decreased integrity of default-mode network in ADHD. *J Neurosci Methods* 2008;169:249-54.
14. Fair DA, Posner J, Nagel BJ, et al. Atypical default network connectivity in youth with attention-deficit/hyperactivity disorder. *Biol Psychiatry* 2010;68:1084-91.
15. Castellanos FX, Margulies DS, Kelly C, et al. Cingulate-precuneus interactions: a new locus of dysfunction in adult attention-deficit/hyperactivity disorder. *Biol Psychiatry* 2008;63:332-7.
16. Castellanos FX, Giedd J, Marsh W, et al. Quantitative brain magnetic resonance imaging in attention deficit hyperactivity disorder. *Arch Gen Psychiatry* 1996;53:607-16.
17. Castellanos FX, Giedd JN, Berquin PC, et al. Quantitative brain magnetic resonance imaging in girls with attention deficit/hyperactivity disorder. *Arch Gen Psychiatry* 2001;58:289-95.
18. Castellanos FX, Lee PP, Sharp W, et al. Developmental trajectories of brain volume abnormalities in children and adolescents with attention-deficit/hyperactivity disorder. *JAMA* 2002;288:1740-8.
19. Peterson BS, Potenza MN, Wang Z, et al. An fMRI study of the effects of psychostimulants on default-mode processing during stroop task performance in youths With ADHD. *Am J Psychiatry* 2009;166:1286-94.
20. Rubia K, Halari R, Cubillo A, et al. Methylphenidate normalises activation and functional connectivity deficits in attention and motivation networks in medication-naïve children with ADHD during a rewarded continuous performance task. *Neuropharmacology* 2009;57:640-52.
21. Brookes MJ, Hale JR, Zumer JM, et al. Measuring functional connectivity using MEG: methodology and comparison with fcMRI. *Neuroimage* 2011a;56:1082-104.
22. Brookes MJ, Woolrich M, Luckhoo H, et al. Investigating the electrophysiological basis of resting state networks using magnetoencephalography. *Proc Natl Acad Sci U S A* 2011;108:16783-8.
23. de Pasquale F, Della Penna S, Snyder AZ, et al. Temporal dynamics of spontaneous MEG activity in brain networks. *Proc Natl Acad Sci U S A* 2010;107:6040-5.
24. Luckhoo H, Hale JR, Stokes MG, et al. Inferring task-related networks using independent component analysis in magnetoencephalography. *Neuroimage* 2012;62:530-41.
25. Fries P. A mechanism for cognitive dynamics: neuronal communication through neuronal coherence. *Trends Cogn Sci* 2005;9:474-80.
26. Schnitzler A, Gross J. Normal and pathological oscillatory communication in the brain. *Nat Rev Neurosci* 2005;6:285-96.
27. Kessler RC, Adler L, Ames M, et al. The World Health Organization Adult ADHD Self-Report Scale (ASRS): a short screening scale for use in the general population. *Psychol Med* 2005;35:245-56.
28. Taulu S, Simola J. Spatiotemporal signal space separation method for rejecting nearby interference in MEG measurements. *Phys Med Biol* 2006;51:1759-68.
29. Taulu S, Simola J, Kajola M. Applications of the signal space separation method (SSS). *IEEE Trans Signal Process* 2005;53:3359-72.
30. Scherg M, Ille N, Bornfleth H, et al. Advanced tools for digital EEG review: virtual source montages, whole-head mapping, correlation, and phase analysis. *J Clin Neurophysiol* 2002;19:91-112.
31. Hoehstetter K, Bornfleth H, Weckesser D, et al. BESA source coherence: a new method to study cortical oscillatory coupling. *Brain Topogr* 2004;16:233-8.
32. Papp N, Ktonas P. Critical evaluation of complex demodulation techniques for the quantification of bioelectrical activity. *Biomed Sci Instrum* 1977;13:135-45.
33. Lachaux JP, Rodriguez E, Martinerie J, et al. Measuring phase synchrony in brain signals. *Hum Brain Mapp* 1999;8:194-208.
34. Wang L, Zhu C, He Y, et al. Altered small-world brain functional networks in children with attention-deficit/hyperactivity disorder. *Hum Brain Mapp* 2009;30:638-49.
35. Cortese S, Kelly C, Chabernaud C, et al. Toward systems neuroscience of ADHD: a meta-analysis of 55 fMRI studies. *Am J Psychiatry* 2012;169:1038-55.
36. Fair DA, Cohen AL, Dosenbach NU, et al. The maturing architecture of the brain's default network. *Proc Natl Acad Sci U S A* 2008;105:4028-32.
37. Stevens MC, Pearlson GD, Calhoun VD. Changes in the interaction of resting-state neural networks from adolescence to adulthood. *Hum Brain Mapp* 2009;30:2356-66.
38. Tian L, Jiang T, Wang Y, et al. Altered resting-state functional connectivity patterns of anterior cingulate cortex in adolescents with attention deficit hyperactivity disorder. *Neurosci Lett* 2006;400:39-43.
39. Tian L, Jiang T, Liang M, et al. Enhanced resting-state brain activities in ADHD patients: a fMRI study. *Brain Dev* 2008;30:342-8.
40. Seidman LJ, Valera EM, Makris N, et al. Dorsolateral prefrontal and anterior cingulate cortex volumetric abnormalities in adults with attention-deficit/hyperactivity disorder identified by magnetic resonance imaging. *Biol Psychiatry* 2006;60:1071-80.
41. Silk TJ, Vance A, Rinehart N, et al. White-matter abnormalities in attention deficit hyperactivity disorder: a diffusion tensor imaging study. *Hum Brain Mapp* 2009;30:2757-65.
42. Shaw P, Eckstrand K, Sharp W, et al. Attention-deficit/hyperactivity disorder is characterized by a delay in cortical maturation. *Proc Natl Acad Sci U S A* 2007;104:19649-54.
43. Shaw P, Lerch J, Greenstein D, et al. Longitudinal mapping of cortical thickness and clinical outcome in children and adolescents with attention deficit/hyperactivity disorder. *Arch Gen Psychiatry* 2006;63:540-9.
44. Makris N, Biederman J, Valera EM, et al. Cortical thinning of the attention and executive function networks in adults with attention-deficit/hyperactivity disorder. *Cereb Cortex* 2007;17:1364-75.